Eur. Phys. J. B **44**, 217–224 (2005)
DOI: 10.1140/epjb/e2005-00117-4

THE EUROPEAN PHYSICAL JOURNAL B

Hund's coupling and the metal-insulator transition in the two-band Hubbard model

Th. Pruschke[1,a] and R. Bulla[2]

[1] Institute for Theoretical Physics, University of Göttingen, Friedrich-Hund-Platz 1, 37077 Göttingen, Germany
[2] Center for Electronic Correlations and Magnetism, Theoretical Physics III, Institute of Physics, University of Augsburg, 86135 Augsburg, Germany

Received 8 November 2004 / Received in final form 22 February 2005
Published online 20 April 2005 –

Abstract. The Mott-Hubbard metal-insulator transition is investigated in a two-band Hubbard model within dynamical mean-field theory. To this end, we use a suitable extension of Wilson's numerical renormalization group for the solution of the effective two-band single-impurity Anderson model. This method is non-perturbative and, in particular, allows to take into account the full exchange part of the Hund's rule coupling between the two orbitals. We discuss in detail the influence of the various Coulomb interactions on thermodynamic and dynamic properties, for both the impurity and the lattice model. The exchange part of the Hund's rule coupling turns out to play an important role for the physics of the two-band Hubbard model and for the nature of the Mott-transition.

PACS. 71.10.Fd Lattice fermion models (Hubbard model, etc.) – 71.27.+a Strongly correlated electron systems; heavy fermions – 71.30.+h Metal-insulator transitions and other electronic transitions

1 Introduction

Many materials with open d- or f-shells show metal-insulator transitions which are commonly classified to be of Mott-Hubbard type due to strong electron-electron correlations [1]. The conventional model to study this type of transition is the one-band Hubbard model [2], which in standard notation reads

$$H = -\sum_{ij\sigma} t_{ij} c^\dagger_{i\sigma} c_{j\sigma} + \frac{U}{2} \sum_{i\sigma} n_{i\sigma} n_{i\bar{\sigma}}. \tag{1}$$

Major progress in understanding the physics of the Mott-Hubbard metal-insulator transition (MHMIT) of the model (1) has been achieved in the last decade through the development of the dynamical mean-field theory (DMFT) [3–5]. At $T=0$ the MHMIT occurs at a critical value of the Coulomb parameter $U_c \approx 1.5W$ [5–7], where W denotes the bandwidth of the density of states at $U=0$. Interestingly, the transition is of first order [5,8] for $T>0$ with a second order end point at a $T_c \approx 0.017W$ and $U_c \approx 1.2W$.

Such a second order end point is also seen in the phase diagram of typical Mott-Hubbard systems like V_2O_3 [9]. Therefore, the one-band Hubbard model has been frequently used as a microscopic model for these materials (see Refs. [5,10] and, in particular, Ref. [11] which focuses on the critical regime close to the second order end point). On the other hand, the justification to base the microscopic description on a one-band model (see Ref. [12]) has been questioned recently [13].

For a proper description of materials such as transition metal oxides, the orbital structure of the relevant electronic degrees of freedom has to be taken into account. This can lead to a fairly complicated form of the underlying tight-binding bandstructure (the kinetic energy term acquires a matrix structure). Furthermore, additional local Coulomb matrix elements arise which describe the interactions between electrons in different orbitals.

The simplest possible extension of the model (1) to the case of orbital degeneracy is the two-band Hubbard model. It is a relevant model whenever the electronic degrees of freedom close to the Fermi level are two-fold degenerate, as for the e_g^σ states in materials like $LaMnO_3$ or $KCuF_3$ [1]. Here we investigate the two-band Hubbard model in the following form:

$$\begin{aligned} H = &-\sum_{ij}\sum_{mm'\sigma} t_{ij}^{mm'} c^\dagger_{im\sigma} c_{jm'\sigma} + \frac{U}{2}\sum_i\sum_{m\sigma} n_{im\sigma} n_{im\bar{\sigma}} \\ &+ \frac{2U'-J}{4}\sum_i\sum_{m\neq m'}\sum_{\sigma\sigma'} n_{im\sigma} n_{im'\sigma'} \\ &- J\sum_i\sum_{m\neq m'} \vec{S}_m \cdot \vec{S}_{m'} \\ &- \frac{J}{2}\sum_i\sum_{m\neq m'}\sum_\sigma c^\dagger_{im\sigma} c^\dagger_{im\bar{\sigma}} c_{im'\bar{\sigma}} c_{im'\sigma}, \end{aligned} \tag{2}$$

[a] e-mail: pruschke@theorie.physik.uni-goettingen.de

with the orbital index $m = 1, 2$. The Coulomb parameters $U' \geq 0$ and $J \geq 0$ describe the inter-orbital Coulomb interaction and Hund's exchange coupling, respectively. The last term in (2) is necessary to ensure rotational invariance of the interaction. By virtue of this rotational invariance the Coulomb parameters are related by $U' = U - 2J$. Generally, the hierarchy of interactions is $U > U' > J$.

A multi-band Hubbard model as in equation (2) displays a Mott transition at all integer fillings (not only at half filling as in the single-band case). The additional Coulomb interactions also modify the value of U_c and, possibly, the character of the transition, as has already been investigated within the DMFT framework [14–18].

Various theoretical and numerical techniques have been employed to investigate multi-band Hubbard models within DMFT. The quantum Monte Carlo method [14,15], which is very successful in treating the multi-band Hubbard models in present applications of the LDA+DMFT approach [19], cannot, however, handle the rotationally invariant form of the interaction in (2) due to the sign problem (for recent progress in reducing this sign problem, see Refs. [20,21]). On the other hand, exact diagonalization [16], linearized DMFT [18] and exact treatments in the limit of infinite orbital degeneracy [17] are not able to reliably calculate dynamical properties.

In this paper, we use Wilson's numerical renormalization group (NRG) [22] to solve the effective two-orbital quantum impurity problem which appears in the DMFT for the two-band Hubbard model. In Section 2 we start with some technical issues related to the NRG in the two-band case. Section 3 shows thermodynamic and dynamic quantities for the two-orbital single-impurity Anderson model, with the focus on the role of the Hund's coupling. In Section 4 we discuss the two-band Hubbard model; here we concentrate on the simplest case, i.e. degenerate orbitals and intra-orbital hopping only: $t_{ij}^{mm'} = t_{ij}\delta_{mm'}$. The model equation (2) is studied on a Bethe lattice (mainly to compare our results with those from other approaches); the generalization to other lattices (other densities of states) is straightforward. The paper is summarized in Section 5.

2 NRG for multi-orbital models

The use of the NRG to solve the effective quantum impurity model appearing in the DMFT self-consistency has been extensively discussed in the literature [7,8,23]. Here we focus on the additional problems arising in the two-orbital impurity Anderson model, which constitutes the effective local model arising in the DMFT for the two-orbital Hubbard model.

The two-orbital Anderson impurity Hamiltonian (in standard notation) is given by

$$\begin{aligned} H = & \sum_{\vec{k}m\sigma} \epsilon_{\vec{k}m\sigma} c^\dagger_{\vec{k}m\sigma} c_{\vec{k}m\sigma} + \sum_{m\sigma} \epsilon_d d^\dagger_{m\sigma} d_{m\sigma} \\ & + \frac{U}{2} \sum_{m\sigma} n^d_{m\sigma} n^d_{m\bar{\sigma}} \\ & + \frac{2U' - J}{4} \sum_{m\neq m'} \sum_{\sigma\sigma'} n^d_{m\sigma} n^d_{m'\sigma'} \\ & - J \sum_{m\neq m'} \vec{S}_m \cdot \vec{S}_{m'} \\ & - \frac{J}{2} \sum_{m\neq m'} \sum_{\sigma} d^\dagger_{m\sigma} d^\dagger_{m\bar{\sigma}} d_{m'\bar{\sigma}} d_{m'\sigma} \\ & \frac{V}{\sqrt{N}} \sum_{\vec{k}m\sigma} c^\dagger_{\vec{k}m\sigma} d_{m\sigma} + \text{h.c.} \end{aligned} \tag{3}$$

Within the NRG approach, the quantum impurity problem is mapped onto a semi-infinite chain form [22] with the impurity at the first site of the chain and the conduction band written in a one-dimensional tight-binding form. The model in the semi-infinite chain form is then solved by iterative diagonalization. Therefore, the major obstacle in applying the NRG to multi-band models is the dramatic increase of the Hilbert space with each NRG step (in each step, one additional site of the semi-infinite chain is included).

A possible solution to this problem is to use very large values of the discretization parameter Λ so that the number of states can be reduced significantly. Averaging over many discretizations (the so-called "Z-trick") has been shown to give reliable results for thermodynamic quantities (see Ref. [24]), even for large values of Λ. However, this approach becomes at least cumbersome for the calculation of dynamic quantities which are required for the DMFT self-consistency.

Here we adopt two different strategies which allow to use a small value of the NRG discretization parameter Λ and to keep enough states in each step so that dynamic quantities can be calculated reliably. The first one is to explicitly include the orbital quantum number in the iterative construction of the basis states. This additional quantum number significantly reduces the typical matrix size, so that O(7000) states can be kept in each NRG iteration with reasonable computation time and memory consumption on modern SMP high-performance computers like e.g. the IBM Regatta. The price to pay is that one has to omit the last term in the Coulomb interaction, i.e.

$$\frac{J}{2} \sum_{m\neq m'} \sum_{\sigma} d^\dagger_{m\sigma} d^\dagger_{m\bar{\sigma}} d_{m'\bar{\sigma}} d_{m'\sigma},$$

because it explicitly breaks the orbital symmetry. However, it turns out that this term does not influence the thermodynamics, and dynamic quantities are only slightly affected via the multiplet structure of the Hubbard bands.

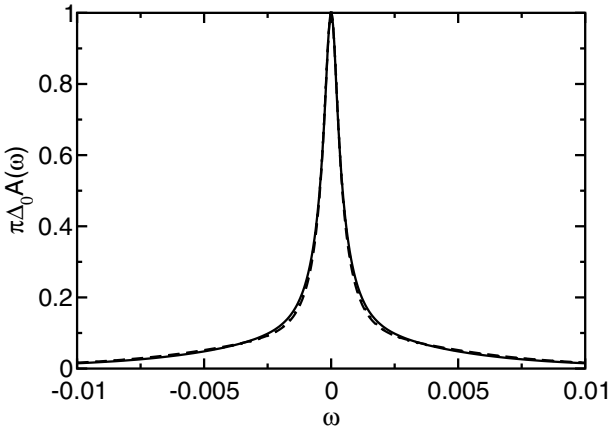

Fig. 1. Comparison of the single-particle dynamics for a NRG calculation (orbitally degenerate and particle-hole symmetric single-impurity Anderson model) in the Kondo regime using the conventional truncation scheme (full line) and the asymmetric truncation scheme (dashed line). Note that particle-hole symmetry and orbital degeneracy are preserved even in the latter scheme.

The second strategy is an asymmetric truncation scheme: instead of adding both orbital degrees of freedom simultaneously, the Hilbert space is truncated after adding each orbital individually. This also leads to a significant reduction of the Hilbert space in the iterative diagonalization.

However, the asymmetric truncation scheme does not guarantee that orbital symmetry is preserved during the NRG iterations. In fact, a slight violation of orbital symmetry is observed for very small energies, typically much lower than the Kondo temperature. It turns out that for the DMFT-calculations presented in Section 4, both methods give almost identical results, at least on the scale shown in the figures.

Figure 1 shows a comparison of the local single-particle density of states (DOS) for the impurity Anderson model equation (3) with twofold degeneracy, particle-hole symmetry, and calculated with both schemes (symmetric truncation with orbital quantum number and asymmetric truncation) in the Kondo limit. Here, the NRG discretization parameter is $\Lambda = 2.5$ and 3600 states were kept in each NRG step. The model parameters are $U = 7\Delta_0$, $J = U/100$ and $U' = U - 2J$. As usual, $\Delta_0 = \pi N_F V^2$ denotes the bare hybridization width (N_F is the conduction electron DOS at the Fermi energy). Obviously, the asymmetric truncation (dashed line) leads to accurate results for both the value of the low-energy scale and the form of the Kondo resonance. In addition, it does not violate particle-hole symmetry and orbital symmetry, at least on the scale shown in Figure 1.

The asymmetric truncation scheme introduced here might be of advantage in cases where the orbital symmetry is violated from the outset so that the orbital quantum number cannot be used in the calculation to reduce the matrix size.

3 Hund's rule coupling in the single-impurity model

Before we turn to the application of the NRG to the two-orbital Hubbard model let us first discuss the effects of Hund's coupling for the single impurity model (3). For simplicity we consider a conduction band with constant DOS, $\rho(\epsilon) = N_F$, in the interval $[-D, D]$ and choose $D = 1$ as unit of energy. The local energy ϵ_d is chosen such that the model is particle-hole symmetric, i.e. $\langle n_d \rangle = 2$. As we will see, there is a profound difference between the cases with rotationally invariant and Ising-like exchange. The two-orbital impurity Anderson model has already been investigated with NRG by several groups [25–27]. Here we want to concentrate on the influence of Hund's coupling on low energy scales and the possibility of a quantum phase transition. To this end we present results for thermodynamic and dynamic properties. To improve the accuracy of thermodynamic properties we employed Oliveira's "Z-trick" [24], which allows to use a larger discretization Λ (we used $\Lambda = 5$) and reduce the number of states kept (1000 after truncation here).

Let us begin with thermodynamic properties of the particle-hole symmetric two-orbital single impurity model in the Kondo limit, that is for a hybridization width $\Delta_0 = \pi N_F V^2$ much smaller than the other bare energy scales [28]. The temperature evolution of the effective squared moment[1] $\mu^2_{eff} := T \cdot \chi_{imp}(T)$ and entropy $S(T)$ for $J = 0$, $U/100$ and $U/10$ is shown in Figure 2. The calculations were done with the rotationally invariant exchange coupling and $U' = U - 2J$, but neglecting the term breaking orbital symmetry. For comparison we also include results for a single-orbital SIAM – marked $m = 1$ in Figure 2 – with the same values of U and Δ_0.

For $J = 0$, i.e. $U = U'$, we observe an intermediate "local-moment regime" with entropy $S = \ln 6$ and effective moment $\mu^2_{eff} = 1/3$ corresponding to the six degenerate states, two of them magnetic, in the atomic limit. As expected from general $SU(N)$ arguments [29] this local moment is eventually Kondo screened with an *enhanced* Kondo scale $\sim \left(T_{\rm K}^{m=1}\right)^{1/m}$. As a technical sidemark let us point out that for $J = 0$, unlike finite J, the asymmetric truncation does *not* work properly, leading to wrong results for S and μ^2_{eff} in the local moment regime.

In the atomic limit, any finite $J > 0$ leads to a spin triplet $S = 1$ as ground state with moment $\langle S_z^2 \rangle = 2/3$ and entropy $\ln 3$. Apparently, this situation is realized for intermediate temperatures for both $J = U/100$ and $J = U/10$. At low temperatures, this local triplet is again quenched by the conduction electrons like for an ordinary $S = 1/2$ Kondo effect. Obviously, the two-orbital system has a considerably reduced low-energy scale $T_{\rm K}$, which in addition decreases strongly with increasing J. At present we do not have a satisfactory explanation for this observation,

[1] The adiabatic effective squared moment $T \cdot \chi_{imp}(T)$ introduced by Wilson [22] should not be confused with the isothermal quantity $\langle S_z^2 \rangle$. Kondo screening can be seen only in the former; the latter goes to a finite constant value as $T \to 0$.

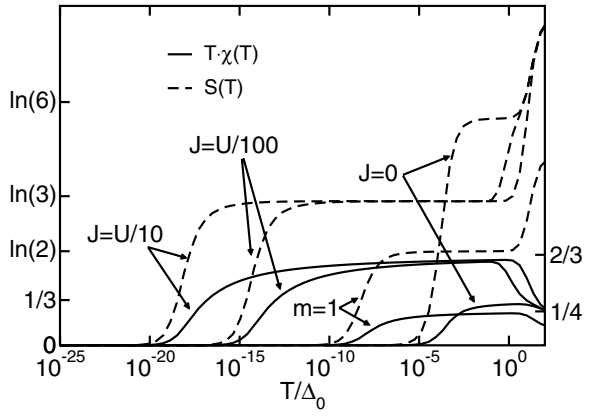

Fig. 2. Thermodynamic properties for a particle-hole symmetric two-orbital impurity model with varying Hund's rule coupling $J = 0$, $U/100$, and $U/10$; dashed lines: entropy, solid lines: effective squared moments. The Coulomb parameter U and the hybridization Δ_0 were chosen such that the system is in the Kondo limit. The inter-orbital Coulomb parameter is fixed to $U' = U - 2J$ by rotational invariance. For comparison the results of a single-orbital SIAM are included.

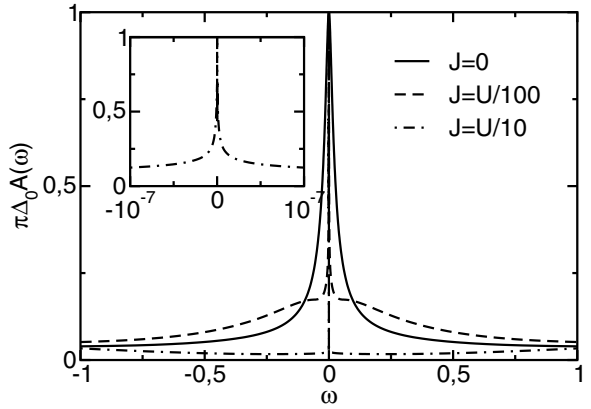

Fig. 3. Local DOS at $T = 0$ for a particle-hole symmetric two-orbital impurity model with Hund's rule coupling $J = 0$, $U/100$ and $U/10$. Other parameters are the same as in Figure 2.

but believe that it is related to the problem how spin-1/2 electrons screen a true $S = 1$ object.

A direct consequence of this substantial reduction of the low-energy scale for the application to the Hubbard model is that critical interactions for an MIT are also strongly reduced for finite J (see Sect. 4 below).

The local DOS at $T = 0$ for $J = U/100$ and $J = U/10$ is shown in Figure 3. The calculations were done with a discretization parameter $\Lambda = 2.5$ and 6400 states kept after truncation. On the scale used in the main panel of Figure 3 the Kondo resonance for $J = U/10$ appears to be a vertical line, pointing to a strongly reduced Kondo temperature, too. In addition, new structures on the scale of J appear as shoulders in the DOS.

If one zooms into the region $[-10^{-7}, 10^{-7}]$ around the Fermi energy (see inset to Fig. 3), only the resonance for $J = U/10$ remains visible with an energy scale well below 10^{-7}. This again confirms the result from the thermodynamic quantities, viz. that with increasing J an exponential reduction of the Kondo temperature occurs. It is quite obvious, that such a reduction in T_K will later manifest itself in a corresponding reduction of the critical U for the Mott-Hubbard metal-insulator transition within the DMFT.

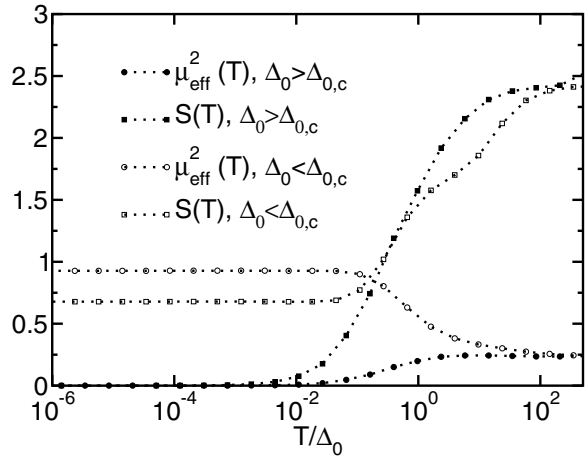

Fig. 4. Comparison of thermodynamic properties for a particle-hole symmetric two-orbital impurity model with Ising-like Hund's rule coupling $J = U/100$ and two values of the hybridization parameter Δ_0. Apparently, there exists a critical $\Delta_{0,c}$ which separates a strong-coupling fixed point ($\Delta_0 > \Delta_{0,c}$) from a local-moment like behaviour ($\Delta_0 < \Delta_{0,c}$).

Let us point out that Friedel's sum rule implies as usual the constraint $\pi\Delta_0 A(0) = 1$. This constraint is fulfilled with high precision due to the calculation of the DOS via the self-energy according to reference [23].

A completely different picture is obtained for an Ising-like exchange interaction in model (3), which is realized by replacing

$$J \sum_{m \neq m'} \vec{S}_m \cdot \vec{S}_{m'} \rightarrow J \sum_{m \neq m'} S^z_m S^z_{m'}$$

and neglecting the term

$$\frac{J}{2} \sum_{m \neq m'} \sum_{\sigma} d^\dagger_{m\sigma} d^\dagger_{m\bar{\sigma}} d_{m'\bar{\sigma}} d_{m'\sigma}.$$

In this case, the atomic ground state is doubly degenerate and consists of the two states where two electrons with the same spin occupy different orbitals. In contrast to the full exchange we find that the properties change quite dramatically with the ratio J/Δ_0, where Δ_0 denotes the hybridization width. In Figure 4 we compare calculations for $J = U/100$ and two different values of Δ_0. For large Δ_0 we find the expected screening and corresponding formation of a Fermi liquid at low temperatures. However, for small Δ_0, this behaviour is replaced by the formation of a state reminiscent of a local moment with entropy $\ln 2$ and effective local moment $\mu^2_{eff} \approx 1$. Obviously, the neglect of the spin-flip terms in Hund's exchange leads to a "critical" ratio $J/\Delta_{0,c}$ separating strong-coupling from local-moment behavior. We interpret this feature in the

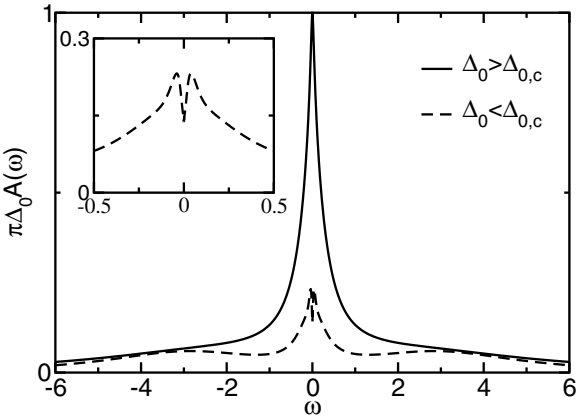

Fig. 5. Comparison of the single-particle dynamics for Ising-like Hund's rule coupling for hybridization strengths above and below the critical $\Delta_{0,c}$. Parameters are the same as in Figure 4.

following way. For the full exchange interaction, spin-flip scattering as in the conventional $S = 1/2$ case is presumably leading to a scenario similar to the standard Kondo effect. For Ising-like Hund coupling J, on the other hand, the atomic ground state consists, as already mentioned, of the two states where two electrons with the same spin occupy different orbitals. Quite apparently, these two states cannot be connected by low-energy processes like spin-flips, i.e. the mechanism leading to the Kondo effect is not present here. However, if the coupling to the band states is large enough such that the $S = 1/2$ Kondo temperature is larger than J, the system can screen the spins for each orbital individually before the coupling J locks the system into the states with $S_z = \pm 1$, leading to the observed strong-coupling behavior at large Δ_0.

Presently, it is not clear whether the change in the impurity properties is connected to some quantum critical behavior like in the pseudo-gap model [30]. The clarification of this question is of course of some interest in its own right and will be discussed in detail in a forthcoming publication.

The impurity DOS corresponding to the two different regimes is shown in Figure 5. For $\Delta_0 > \Delta_{0,c}$ (full line) the typical structure is obtained. Decreasing Δ_0 below $\Delta_{0,c}$ completely changes the structure of the DOS. Instead of a Kondo peak, we now find a structure with a pseudo-gap at the Fermi energy. It is quite evident, that this "criticality" in the impurity model has profound effects on the MIT in the DMFT calculations for the Hubbard model.

4 MIT in the two-orbital Hubbard model

Theoretical investigations of multi-orbital Hubbard models within DMFT have already led to a better understanding of various issues such as the nature of the Mott-transition as a function of orbital degeneracy [14–18,31] and the structure of the spectral function in realistic treatments within the LDA+DMFT approach [19]. Detailed results have been obtained for the dependence of the critical interaction strength U_c on the number of orbitals M and different integer fillings n. Numerical DMFT-QMC calculations have been performed for $M \leq 3$ [14,15,32]. Remarkably, in the limit of large orbital degeneracy $M \to \infty$ an analytical treatment of the DMFT becomes possible for the MIT [17]. For $T = 0$, a scaling $U_c = U_{c,2} \propto M$ for the actual transition is found while $U_{c,1} \propto \sqrt{M}$ is obtained for the critical interaction where the insulating solution breaks down [17]. This is consistent with the linear dependence for large M found in references [18,33,34] and with the square-root dependence reported in reference [35]. The inclusion of the Hund's rule exchange coupling J has been shown to significantly reduce the value of U_c [15,18,35]. In particular, a qualitative change from continuous for $J = 0$ to discontinuous for any finite J has been observed in reference [18] (see also the Gutzwiller results in Ref. [36]). A significant quantitative change of U_c when excluding the spin-dependent part from the exchange coupling in equation 2 has already been mentioned in reference [18], but detailed results have not been published yet. Recently, the issue of possible orbital-selective Mott transitions has been investigated in references [37,38].

Let us now discuss the results from the NRG for the particle-hole symmetric case. To allow a direct comparison with earlier results, we use as non-interacting DOS the semielliptic form $\rho_0(\omega) = \frac{2}{\pi}\sqrt{1-\omega^2}$ (Bethe lattice) with the same bandwidth for both orbitals. As NRG discretization parameter we choose $\Lambda = 2.5$ and keep 6400 states after truncation.

Except for $J = 0$, all the following results were obtained with the asymmetric truncation scheme introduced in Section 2 including all Coulomb interactions from the model (2). We have observed that the symmetric truncation scheme (taking into account the orbital quantum number and neglecting the last term in the interaction) leads to identical results for spectral functions, apart from some weak redistribution of spectral weight in the Hubbard bands due to a different atomic multiplet structure. However, the latter effect is only barely noticeable due to the broadening introduced in calculating continuous spectra from the NRG. More important, the critical values U_c for all two-band calculations within DMFT are not affected; possible problems due to the breaking of orbital symmetry by the asymmetric truncation scheme do not play a role here, except again for $J = 0$.

We begin by comparing results for the one-band Hubbard model (1) (Fig. 6a) and a two-orbital Hubbard model with $J = 0$ and $U = U'$ (Fig. 6b). As is well-known from earlier DMFT calculations [14,15], the critical Coulomb parameter, U_c, for the model with $J = 0$ increases strongly with the orbital degeneracy M, $U_c \sim M$ [17,18]. This is also apparent from the results in Figure 6b. The system stays metallic up to the largest U shown. The actual MIT occurs for a value $2.5W < U_c \lesssim 3W$.

The results in Figures 6 and 7 are calculated with a fairly large value of $\Lambda = 2.5$ and broadening parameter $b = 0.8$ (see Eq. (8) in Ref. [8]) for both the single-band case in Figure 6a and the two band case in Figures 6b and 7. We therefore expect that our critical values U_c for

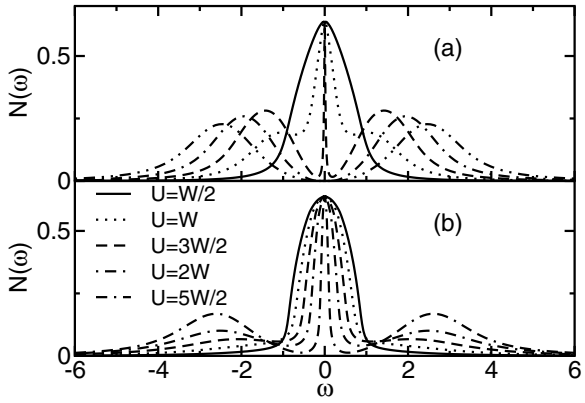

Fig. 6. (a) Development of the DOS as function of U for (a) one-band model equation (1) and (b) two-orbital model equation (2) with $J = 0$ and $U = U'$.

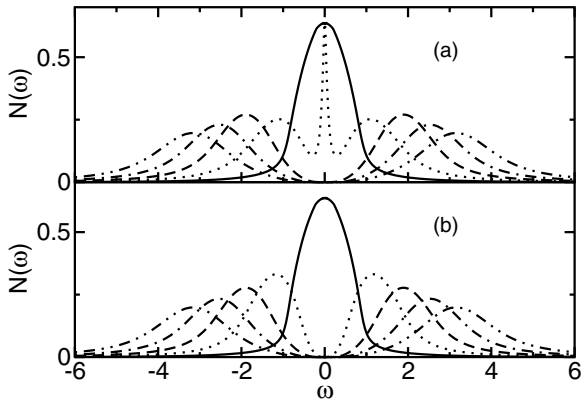

Fig. 7. Development of the DOS as function of U for the two-orbital model with (a) full $J = U/4$ and (b) two-band model with Ising-like $J = U/4$. In both cases $U' = U - 2J$ was used. The assignment between the different line styles and values of U is the same as in Figure 6.

the Mott transition differ from more precise calculations, and indeed we find them to be somewhat overestimated. In the single-band case, for example, our result for $U_c \approx 1.6W$ is slightly (10%) larger than the well established value $U_c = 1.47W$ [7]. A similar overestimation is also present for $M = 2$, where $U_c \lesssim 2.5W$ is reported in the literature [14–18]. However, the qualitative features of the transition are not altered by this overestimation.

The influence of Hund's coupling on the development of the spectra and the occurrence of the MIT can be seen in Figure 7a, where results for different values of U and a full Hund's exchange $J = U/4$ are presented [39]. As has been noted before [16,18], finite J substantially reduces U_c. Such a behavior is also seen in Figure 7a. The critical Coulomb parameter is reduced from $U_c \approx 3W$ for $J = 0$ to $U_c \approx 1.1W$.

Presently, the standard technique to solve quantum impurities with orbital degeneracy is quantum Monte-Carlo (QMC). However, due to the minus sign problem, one has to restrict the Coulomb interaction to density-density type only, i.e. an Ising-like Hund's exchange. The last term in (2) has to be neglected completely. This raises

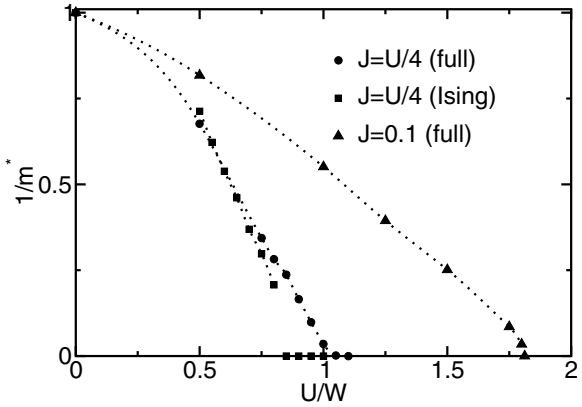

Fig. 8. Inverse effective mass as function of U/W and $J = U/4$ for the full (circles) and Ising-like exchange interaction (squares). The latter shows a strong jump in $1/m^*$ at U_c, leading to a first order transition, while the former vanishes continuously. The triangles represent a calculation with fixed $J = 0.1$. The lines are meant as guide to the eyes.

the following questions: What are the consequences of this approximation for the dynamics and in particular the MIT?

To answer this question (at least partially) we performed calculations with Ising-like exchange interaction as defined in the previous section (see Ref. [40]) The results are shown in Figure 7b. At a first glance, the results are not very different, except that the critical U is further reduced to $U_c \approx 0.8W$. On the other hand, the results for the impurity calculation in Figures 4 and 5 already indicate that the replacement of Hund's exchange by an Ising-like term has more severe consequences than a mere quantitative change of energy scales. In the following we show that this approximation indeed leads to a qualitative change in the physical properties of the Mott-Hubbard MIT.

Let us now turn to the nature of the Mott transition. For a one-band model, it is now commonly accepted that the transition is of second order at $T = 0$ with a quasiparticle weight that vanishes smoothly as one approaches U_c. There is, however, a substantial region below U_c, where the insulator is metastable [5,7]. Previous work using the so-called linearized DMFT (L-DMFT) suggests that for orbitally degenerate systems with finite J this may be different [18]. The authors of reference [18] found a first order transition for small to intermediate J signaled by a jump in the quasiparticle weight at U_c. The NRG results for the inverse effective mass ($\equiv$ quasiparticle weight) for the case $J = U/4$ are shown in Figure 8. The circles were obtained from calculations using the full interaction, while the squares represent calculations with Ising-like interactions. Apparently, the latter signal a strong first order transition at $U_c \approx 0.8W$, while the former lead to a continuously vanishing quasiparticle weight. For a fixed $J = 0.1$ (triangles in Fig. 8) the quasi-particle weight near U_c also shows a jump at U_c as predicted by L-DMFT [18]. However, the magnitude of this jump comes out much smaller in our calculations.

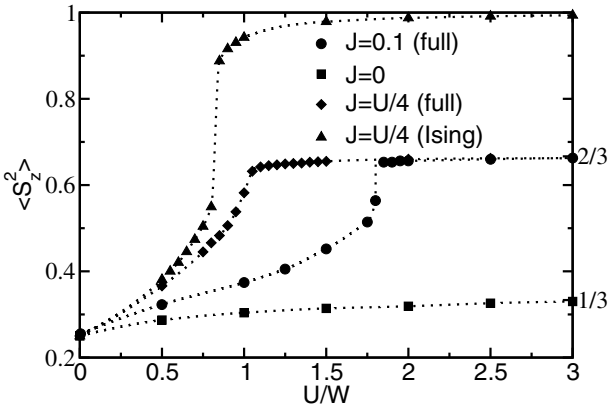

Fig. 9. $\langle S_z^2 \rangle$ for the two-band Hubbard model and different values of J. The lines are meant as guide to the eye. Note that for $J = 0.1$ and Ising-like $J = U/4$ a discontinuity in $\langle S_z^2 \rangle$ occurs at the critical U.

The differences between the different calculations ($J = 0$, $J = 0.1$ and $J = U/4$) become more apparent when one looks at the local squared moment $\langle S_z^2 \rangle$. For $U \to 0$ this quantity has the value $\langle S_z^2 \rangle = 1/4$ (for $J = 0.1$ it is actually slightly larger), while deep in the Mott insulator it acquires the atomic value enforced by Hund's coupling, i.e. $\langle S_z^2 \rangle = 1/3$ for $J = 0$, $\langle S_z^2 \rangle = 2/3$ for finite full J and $\langle S_z^2 \rangle = 1$ for Ising-like J. This behavior is readily found in the calculated values of $\langle S_z^2 \rangle$ in Figure 9. In accordance with the results presented in reference [18], the limiting value for $\langle S_z^2 \rangle$ is approached smoothly for $J = 0$. The same holds for $J = U/4$, consistent with the results for the quasi-particle weight in Figure 8. The slope, however, strongly increases when one approaches U_c from below. For constant $J = 0.1$, the numerical results are not decisive, and could be interpreted as both a small discontinuity at U_c and a continuous approach with diverging slope. On the other hand, a quite strong discontinuity at U_c appears for an Ising-like Hund's coupling $J = U/4$, signalling a rather strong first order transition in this case. The above results are in rough agreement with the L-DMFT predictions [18], although there one observes a first-order transition also for smaller values of J.

The appearance of an unambiguous and rather strong first order transition for an Ising-like exchange coupling shows that in this case the physics underlying the Mott-Hubbard transition is very different from the one for the rotationally invariant exchange interaction. As for the single impurity model, we believe that a transition between individually screened orbitals on the metallic side to a local-moment regime enforced by the Ising coupling on the insulating side occurs as soon as J becomes of the order of the Fermi liquid scale. Depending on the details of the non-interacting DOS (its value at the Fermi level and the band width) and the values of U and J, this can lead in the worst case to a serious underestimation of U_c and possibly an incorrect description of the behavior of physical quantities close to the transition.

5 Summary and conclusions

In this paper we presented first studies of the Mott-Hubbard transition in a two-orbital Hubbard model within the DMFT at $T = 0$ using Wilson's NRG. In addition to a standard NRG implementation using the orbital quantum number, we proposed an asymmetric truncation scheme which turns out to work rather well in both the two-orbital single impurity Anderson model and the two-band Hubbard model.

As a first interesting result, we observed that for the particle-hole symmetric case a finite Hund's exchange $J > 0$ leads to a tremendous reduction in the low-energy scale $T_{\rm K}$. This is in striking contrast to the result for $J = 0$, i.e. $U = U'$, where the behavior conventionally expected for an $SU(N)$ Kondo model, viz. $T_{\rm K} \sim \sqrt[N]{T_{\rm K}^{N=1}}$, is found [29]. At present, the precise theoretical reason for this rather unexpected strong influence of J on $T_{\rm K}$ is not clear. Interestingly, it is also rather different from the case $\langle n_d \rangle \approx 1$ where we find a mild *increase* of $T_{\rm K}$ with increasing J. Obviously, a detailed study of the physics of multi-orbital quantum impurity models has to be an important future aim.

A completely different behavior occurs if one replaces the rotationally invariant Hund exchange by an Ising-like one. In this case, the levels of the atomic doublet with $S_z = \pm 1$ enforced by the Ising coupling cannot be connected by Schrieffer-Wolff type spin-flip processes. Thus, the Kondo effect can only occur for $J \leq T_{\rm K}^{m=1}$, while for larger J the systems is locked into a local moment enforced by the exchange coupling. Note that this interpretation also implies that in the strong-coupling phase the spins on each individual orbital will be screened separately, while for the rotationally invariant case a full $S = 1$ system must be screened. The details of the quantum phase transition between strong-coupling and local moment phases have not yet been analyzed. However, in view of a possible relevance of an Ising-anisotropy in the presence of crystal fields, a further investigation of this problem is certainly interesting.

We also applied the NRG to the two-orbital Hubbard model in the framework of DMFT to investigate the Mott-Hubbard metal-insulator transition at $T = 0$ for the half-filled case. The major goal was here to eludicate the influence of Hund's coupling on the MIT and to investigate how the restriction to an Ising-like exchange changes the nature of the MIT. Our results are in general agreement with previous ones [14–18]. In particular, for finite J quantities like the effective mass or $\langle S_z^2 \rangle$ show diverging slopes as $U \nearrow U_c$, possibly even discontinuities as proposed by the L-DMFT [18].

For an Ising-like Hund's exchange coupling the situation becomes qualitatively different. As can be anticipated from the behavior of the impurity model, the MIT is strongly first order with clear jumps in the effective mass and $\langle S_z^2 \rangle$. Note that the former also implies a discontinuous vanishing of the quasi-particle peak at $T = 0$ as one reaches U_c. Also the physics underlying this transition is quite different compared to the rotationally invariant case,

reflecting the lack of spin-flip scattering processes connecting the two states $S_z = \pm 1$. Thus, the metallic phase with Ising-like interaction will be characterized by individual screening of the spins on the two orbitals rather than a Kondo screening of a total spin $S = 1$. Note that this subtlety will most likely influence low-energy properties on the metallic side close to U_c, but be less important for "high-energy" properties like magnetic or orbital ordering.

It is clear, that the investigations presented here are merely a starting point to systematically study properties of multi-orbital impurity models or correlated lattice models within the DMFT at $T \to 0$ using Wilson's NRG. The major advantage of this method is obviously its unmatched ability to handle exponentially small energy scales and nevertheless provide reliable information on dynamics and thermodynamics even on high-energy scales. Thus, at least for two-orbital models we are now in a position to systematically study their physical properties and address questions that are of fundamental interest for a realistic description of, for example, transition metal oxides but require local degrees of freedom beyond a simple one-band Hubbard model.

We acknowledge useful conversations with F. Anders, A. Lichtenstein, M. Vojta, and D. Vollhardt. This work was supported by the DFG through the collaborative research center SFB 484, the Leibniz Computer center, the Computer center of the Max-Planck-Gesellschaft in Garching and the Norddeutsche Verbund für Hoch- und Höchstleistungsrechnen.

References

1. M. Imada, A. Fujimori, Y. Tokura, Rev. Mod. Phys. **70**, 1039 (1998)
2. J. Hubbard, Proc. R. Soc. London A **276**, 238 (1963); M.C. Gutzwiller, Phys. Rev. Lett. **10**, 159 (1963); J. Kanamori, Prog. Theor. Phys. **30**, 275 (1963)
3. W. Metzner, D. Vollhardt, Phys. Rev. Lett. **62**, 324 (1989)
4. T. Pruschke, M. Jarrell, J.K. Freericks, Adv. Phys. **42**, 187 (1995)
5. A. Georges, G. Kotliar, W. Krauth, M.J. Rozenberg, Rev. Mod. Phys. **68**, 13 (1996)
6. M. Jarrell, Th. Pruschke, Z. Phys. B **90**, 187 (1993)
7. R. Bulla, Phys. Rev. Lett. **83**, 136 (1999)
8. R. Bulla, T.A. Costi, D. Vollhardt, Phys. Rev. B **64**, 045103 (2001)
9. D.B. McWhan, J.P. Remeika, Phys. Rev. B **2**, 3734 (1970); D.B. McWhan et al., Phys. Rev. B **7**, 1920 (1973)
10. M.J. Rozenberg et al., Phys. Rev. Lett. **75**, 105 (1995)
11. P. Limelette, A. Georges, D. Jérome, P. Wzietek, P. Metcalf, J.M. Honig, Science **302**, 89 (2003)
12. C. Castellani, C.R. Natoli, J. Ranninger, Phys. Rev. B **18**, 4967 (1978); C. Castellani, C.R. Natoli, J. Ranninger, Phys. Rev. B **18**, 5001 (1978)
13. S. Yu. Ezhov, V.I. Anisimov, D.I. Khomskii, G.A. Sawatzky, Phys. Rev. Lett. **83**, 4136 (1999)
14. M.J. Rozenberg, Phys. Rev. B **55**, R4855 (1997)
15. J.E. Han, M. Jarrell, D.L. Cox, Phys. Rev. B **58**, 4100 (1998)
16. A. Koga, Y. Imai, N. Kawakami, Phys. Rev. B **66**, 165107 (2002)
17. S. Florens, A. Georges, G. Kotliar, O. Pacollet, Phys. Rev. B **66**, 205102 (2002)
18. Y. Ōno, M. Potthoff, R. Bulla, Phys. Rev. B **67**, 035119 (2003)
19. G. Kotliar, D. Vollhardt, Physics Today **57**, No. 3 (March), 53 (2004); K. Held, I.A. Nekrasov, G. Keller, V. Eyert, N. Blümer, A.K. McMahan, R.T. Scalettar, Th. Pruschke, V.I. Anisimov, D. Vollhardt, Psi-k Newsletter #56, 65 (2003) [`psi-k.dl.ac.uk/newsletters/News_56/Highlight_56.pdf`]
20. S. Sakai, R. Arita, H. Aoki, Phys. Rev. B **70**, 172504 (2004)
21. A.N. Rubtsov, V.V. Savkin, A.I. Lichtenstein, `cond-mat/0411344` (2004)
22. K.G. Wilson, Rev. Mod. Phys. **47**, 773 (1975); H.R. Krishna-Murthy, J.W. Wilkins, K.G. Wilson, Phys. Rev. B **21**, 1003 (1980); H.R. Krishna-Murthy, J.W. Wilkins, K.G. Wilson, Phys. Rev. B **21**, 1044 (1980)
23. R. Bulla, A.C. Hewson, Th. Pruschke, J. Phys.: Condens. Matter **10**, 8365 (1998)
24. W.C. Oliveira, L.N. Oliveira, Phys. Rev. B **49**, 11986 (1994)
25. O. Sakai, Y. Shimizu, T. Kasuya, J. Phys. Soc. Jpn **58**, 3666 (1989); W. Izumida, O. Sakai, Y. Shimizu, J. Phys. Soc. Jpn **67**, 2444 (1998)
26. M. Kojima, S. Yotsuhashi, K. Miyake, Acta Phys. Pol. B **22**, 1331 (2003); L. De Leo, M. Fabrizio, Phys. Rev. B **69**, 245114 (2004)
27. A.K. Zhuravlev, V.Y. Irkhin, M.I. Katsnelson, A.I. Lichtenstein, Phys. Rev. Lett. **93**, 236403 (2004)
28. The quarter-filled case is, as far as Hund's coupling is concerned, of little interest here. However, interesting physics can be found in the presence of a magnetic field (see, for example, Ref. [27])
29. A.C. Hewson, *The Kondo Problem to Heavy Fermions* (Cambridge University Press, 1993)
30. R. Bulla, M. Vojta, in *Concepts in Electron Correlations*, edited by A.C. Hewson, V. Zlatic (Kluwer Academic Publishers, Dordrecht, 2003), p. 209; and references therein
31. G. Kotliar, H. Kajueter, Phys. Rev. B **54**, 14221 (1999)
32. A. Koga, T. Ohashi, Y. Imai, S. Suga, N. Kawakami, J. Phys. Soc. Jpn **72**, 1306 (2003)
33. J.P. Lu, Phys. Rev. B **49**, 5687 (1994)
34. R. Frésard, G. Kotliar, Phys. Rev. B **56**, 12909 (1997); R. Frésard, M. Lamboley, J. Low Temp. Phys. **126**, 1091 (2002)
35. E. Koch, O. Gunnarsson, R.M. Martin, Phys. Rev. B **60**, 15714 (1999)
36. J. Bünemann, W. Weber, Phys. Rev. B **55**, 4011 (1997); J. Bünemann, W. Weber, F. Gebhard, Phys. Rev. B **57**, 6896 (1998)
37. A. Koga, N. Kawakami, T.M. Rice, M. Sigrist, Phys. Rev. Lett. **92**, 216402 (2004)
38. A. Liebsch, Phys. Rev. Lett. **91**, 226401 (2003)
39. We have chosen a fixed ration for J/U, because in typical experiments we expect the bandwidth to be the control parameter (through the variation of pressure); this means it is more natural to change U/W and J/W, but keep J/U fixed
40. Neglect of last term in (2) in fact appears to be non-critical. We therefore concentrate of the spin-flip terms in Hund's coupling